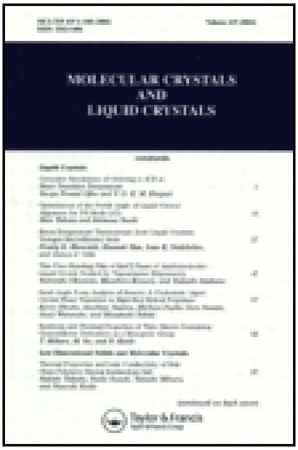

Molecular Crystals and Liquid Crystals
Publication details, including instructions for authors and subscription information:
http://www.tandfonline.com/loi/gmcl20

In Situ Second Harmonic Generation in Disperse Red 1-Doped Polymer and Sol-Gel Films

A. Samoc [a], M. Samoc [a], B. Luther-Davies [a], V. Z. Kolev [a], R. K. Bagien [a], X. Luo [a] & C. Zha [a]

[a] Laser Physics Centre, Research School of Physical Sciences and Engineering, The Australian National University, Canberra, Australia

To cite this article: A. Samoc, M. Samoc, B. Luther-Davies, V. Z. Kolev, R. K. Bagien, X. Luo & C. Zha (2006): In Situ Second Harmonic Generation in Disperse Red 1-Doped Polymer and Sol-Gel Films, Molecular Crystals and Liquid Crystals, 446:1, 123-140

To link to this article: http://dx.doi.org/10.1080/15421400500383360

Mol. Cryst. Liq. Cryst., Vol. 446, pp. 123–140, 2006
Copyright © Taylor & Francis Group, LLC
ISSN: 1542-1406 print/1563-5287 online
DOI: 10.1080/15421400500383360

In Situ Second Harmonic Generation in Disperse Red 1-Doped Polymer and Sol-Gel Films

A. Samoc
M. Samoc
B. Luther-Davies
V. Z. Kolev
R. K. Bagien
X. Luo
C. Zha
Laser Physics Centre, Research School of Physical Sciences and Engineering, The Australian National University, Canberra, Australia

We investigated linear optical and second-order nonlinear optical (NLO) properties of films of poly(bisphenol A carbonate) resin, and a newly synthesised titania/silica/hybrid sol-gel polymer resin doped with Disperse Red 1 (DR1) molecular chromophore. DC electric field induced second harmonic generation (SHG) technique has been used to monitor in situ the polar alignment and relaxation of orientation of the guest molecules in the corona-poled films. The temporal behaviour of the second harmonic signal was remarkably different in these two polymers both during poling and when the poling field was turned off. A fast decay of the second harmonic intensity was observed at room temperature in 3 wt% DR1-doped sol-gel film, and a long relaxation time constant was found in 13 wt% DR1-doped polycarbonate film. Resonantly enhanced d_{eff} *coefficient of about 9 pm/V was found in the sol-gel film, and 25 pm/V in the polycarbonate film at the fundamental wavelength 1053 nm. The* d_{33} *values were about 20 pm/V, and 60 pm/V in these films, respectively. The SHG results were used to estimate the average rotation mobility parameter of DR1 molecules in the host polymers.*

Keywords: benchmark NLO dye; bisphenol-A polycarbonate; organomineral resin; orientation order dynamics; rotation mobility parameter; SHG

Support from the Australian Photonics CRC and the Australian Research Council and technical help of M. Pennington are gratefully acknowledged.

Address correspondence to A. Samoc, Laser Physics Centre, Research School of Physical Sciences and Engineering, The Australian National University, Canberra ACT 0200, Australia. E-mail: anna.samoc@anu.edu.au

INTRODUCTION

Second-order nonlinear optical (NLO) polymeric materials can be attractive candidates for electro-optic modulation of laser light and for sensing applications if they show large second-order nonlinear optical macroscopic susceptibility $\chi^{(2)}$, have good thermal and photochemical stability (high glass transition temperature T_g) in addition to the ease of processing into films or optical fibres. Such materials need to form a structure in a non-centrosymmetric space group either spontaneously or through assembling the molecules in a polar order by external means [1]. One possible approach towards the preparation of the prospective materials is by selecting molecules of high hyperpolarizability β and embedding them into a suitable matrix in a polar order to optimise their nonlinear properties. Such a strategy can lead to various degrees of utilization of the molecular hyperpolarizabilities. A full contribution of the hyperpolarizability to the macroscopic nonlinear susceptibility can be realised, for example, in the family of spontaneously formed non-centrosymmetric, second-order highly nonlinear uniaxial crystals of molecular complexes of triiodides [2–5]. Presumably, weak intermolecular interactions play an important role in the packing of adduct molecules into this stable, non-centrosymmetric orientation arrangement in which all triiodide dipoles are positioned parallel to the polar axis direction.

A partial polar alignment of NLO species can be achieved with the methods of electrical, optical and mechanical poling. The electrical poling is a convenient method of aligning of dipolar molecules by applying an electric field to the material sandwiched between parallel plate electrodes, or in a corona setup [6,7]. The poling is followed by permanent or quasi-permanent fixing of the induced alignment of dipoles resulting in formation of the medium of $C_{\infty v}$ symmetry. The alignment induced second-order nonlinear susceptibility depends on the orientation factor $O(\Theta, \phi)$ following Eq. (1) [8]

$$\chi^{(2)}(-2\omega;\omega,\omega) = N\beta f(2\omega)f(\omega)f(\omega)O(\Theta,\phi) \tag{1}$$

where Θ and ϕ are polar angles between the molecule dipole moment and the poling field, N is the number density, f is the local field factor. The $\chi^{(2)}_{\mathrm{ijk}}$ tensor elements can be modified by the polar order orientation functions expressed through $\langle\cos(\Theta)\rangle$ and $\langle\cos^3(\Theta)\rangle$ [8–10]. The tensor components can be monitored by measuring the intensity of the second harmonic, $I^{2\omega}$, since $I^{2\omega} \propto |(\chi^{(2)})|^2$. In the corona poling experiments the poling field is applied along the laboratory axis 3, parallel to the normal to the film. The $\chi_{333}{}^{(2)}$ tensor elements and the second harmonic coefficients d_{333}, depend on the order parameter expressed as a function of

$\langle \cos^3(\Theta) \rangle$. During the poling process the polymer is heated to the glass transition temperature T_g to reduce viscosity and facilitate an easier rearrangement of molecules. The change in orientation of molecules due to poling can be probed with second harmonic generation as well as the EO effect [11,12]. Other sensitive tools useful for evaluation of the orientational order parameter and stability of the alignment are the linear spectroscopy, which monitors changes in anisotropy of absorption [7]. and the refractive index measurements for monitoring changes in a birefringence of the films and waveguiding [13].

The orientation dynamics of the chromophore dipoles can be quantified with the average rotation mobility parameter $\rho(T)$ [10] at temperature T, defined by Eq. (2)

$$\rho(T) = \frac{\langle \cos^3(\Theta) \rangle_T}{\langle \cos^3(\Theta) \rangle_{\text{free}}} \tag{2}$$

This parameter can vary from 0 for dipoles unable to rotate in an electric field to 1 for free rotating dipoles, unconstrained at sufficiently high temperature. It can be determined from the ratio of the second harmonic intensity from the polymer at a temperature T_1 to that at temperature $T_2 > T_g$.

We used the *in situ* SHG technique for a real-time monitoring of the changes of the second-order susceptibility during corona poling and on removal of the poling field. The purpose of this work was to align molecules and observe relaxation of polar orientation of the relatively large (sub-nm^3 size) molecule of the benchmark NLO chromophore, Disperse Red 1 (DR1), in films of two different hosts: a commercial polycarbonate resin, and a newly synthesised titania/silica/hybrid polymer resin.

EXPERIMENTAL

The dye-doped polymer films were corona poled while the second harmonic signals, produced by passing through the sample a laser beam of the wavelength 1053 nm from an amplified mode-locked Nd:YLF pulsed laser system, were acquired as a function of time, sample temperature and poling field. The NLO susceptibility coefficients, d_{eff}, and d_{33}, were determined from the Maker-fringe method [14,15]. Relaxation parameters of the reorientation of the dye molecules after poling have been obtained from the analysis of the change of the coefficient d_{33} with time. The SHG wavelength of 526.5 nm was very close to the absorption maximum of the dye in the host polymers, thus the second harmonic was strongly absorbed and the nonlinearity was resonantly enhanced.

Materials

The guest-host systems of polycarbonate (PC) resin and the sol-gel titania/silica/hybrid polymer resin, $[Si(C_6H_5)_2O]_x(TiO)_y(MPS)_z$, were doped with Disperse Red 1 (DR1) of 95% purity, used as received. Figure 1 shows molecular structures of the studied materials.

Polycarbonate (PC) Resin

The host polymer, poly(bisphenol A carbonate) resin (Aldrich, 18,162–5) of density 1.2 g/cm^3, average molecular weight ca. 64,000 was chosen for its good film forming ability using chlorinated solvents. The DR1 dye could be mixed with the polymer host in a wide range of the dye concentrations, up to 20–25 wt% (the dye and the polymer were dissolved in separate solutions then mixed together). Uniform, high optical quality films having thicknesses in the range 1–2 µm were prepared on ITO-coated glass microscope slides for the SHG measurements. A filtered solution of the 13 wt% DR1-doped polymer (about 10 wt% of PC) in 1,1,2,2-tetrachloroethane was used for spin coating

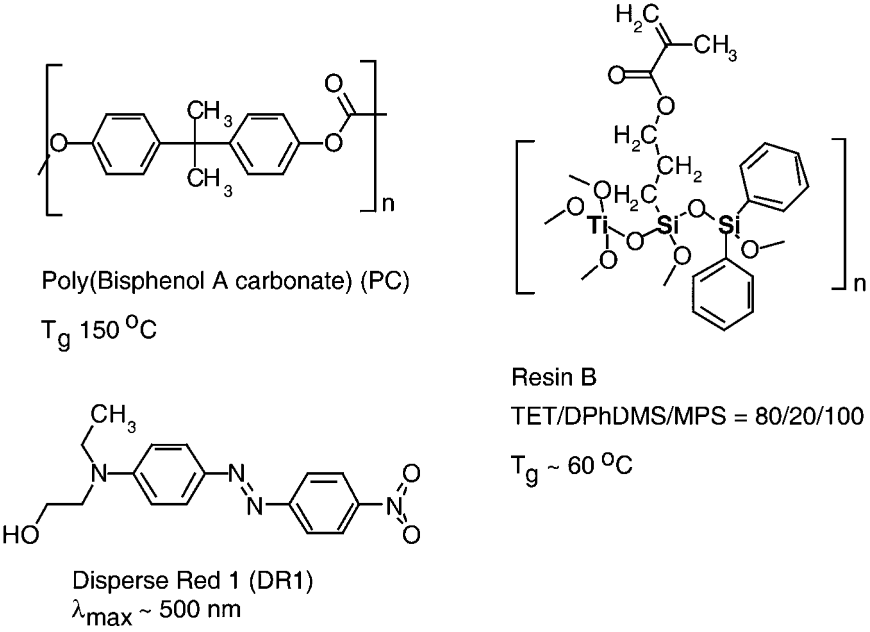

FIGURE 1 Molecular formulae of components of the guest-host systems: polycarbonate, and the sol-gel resin B - the hosts, Disperse Red 1 – the guest NLO dye.

of the substrates using a Headway spinner and dried under vacuum at 70°C.

The refractive index, $n_D^{20} = 1.5850$ of neat polycarbonate resin is suitable for preparing slab optical waveguides using common glass substrates. An attractive important feature of the neat PC polymer is its high value of the glass transition temperature, $T_g = 150°C$. This temperature is remarkably higher than in the commonly studied polymer host, poly(methylmethacrylate) (PMMA) where the T_g is near 105°C.

Sol-gel (SG) Hybrid Resin

The polymer resin of the formula $[Si(C_6H_5)_2O]_x(TiO)_y(MPS)_z$, shown in Figure 1, was prepared by an anhydrous sol-gel process from the following components: diphenyldimethoxysilane (DPhDMS), titanium(IV) ethoxide (TET) and [3-(methacryloyloxy)propyl]trimethoxysilane (MPS), in a two-step synthesis similar to the one described in Ref. [16].

In the first step the MPS alkoxide was hydrolysed in the reaction (1). The hydrolysis was performed in methanol by mixing the components, MPS:boric acid in a proportion 1:0.5–1:1. The reaction proceeded under reflux conditions (2 hours) allowing for the exchange of ligand methoxy groups of MPS with the hydroxy group (OH) of boric acid. The volatile product $B(OCH_3)_3$ and the solvent were evaporated under vacuum (400 mbar at 80°C for 30 min) giving a highly viscous product, the resin A.

In the second step the condensation reaction (2) was accomplished with DPhDMS and TET added to the resin A in the proportion of DPhDMS/TET/ MPS molar ratio 80/20/100. The mixture was refluxed (80°C, 1hour) under nitrogen. The by-products of the condensation reaction such as methanol and ethanol were removed with a rotary evaporator (80°C under vacuum 1 mbar). The viscous product, the titania/silica/hybrid polymer resin (B), was filtered with a membrane (0.2 μm pores) filter.

Films of the 3 wt% DR1-doped organomineral hybrid polymer resin were prepared from the cyclohexanone solution of the resin B, mixed with cyclohexanone solution of DR1, and filtered. Films, of the thickness 1–2 μm, were prepared by spin-coating of bare glass slides and an ITO-coated glass substrate and dried in air at 80°C for about 20 min.

Measurement Techniques

Absorption of light in the DR1-doped films was measured in the UV-vis-near infrared range with Shimadzu (UV-3101PC) and Varian Carry 5000 spectrophotometers. Film thickness was measured with a Utencor Alpha-step profilometer, and compared with the data obtained from a Metricon prism coupler (model 2010). Refractive indices were measured using the prism coupler at 632.8 nm, 814 nm, and 1064 nm wavelengths.

Second harmonic generation was measured using the Maker fringe technique. The experimental setup consisted of a sample holder, a corona poling rig, an in-house built amplified mode-locked pulsed laser system operating at the fundamental wavelength of 1053 nm, the second harmonic and temperature detection and recording systems.

The pulsed laser system consisted of a diode-end-pumped 1053 nm Nd:YLF laser oscillator [17], mode-locked with a semiconductor saturable absorber mirror (SESAM). The SESAM was grown using low-pressure metal-organic chemical vapor deposition (MOCVD) technique. The saturable absorption of the device was provided by two InGaAs quantum wells and the design was similar to the one described in Ref. [18]. Employing temperature tuning of the SESAM as a means to control the modulation depth resulted in stable continuous wave (cw) mode-locked operation. A train of 6 ps pulses at 25 MHz repetition rate was generated with an average power of 500 mW. The laser had excellent beam quality ($M^2 < 1.1$) and long-term stability. This laser oscillator was coupled to a Nd:YLF regenerative amplifier operating at 20 Hz repetition rate, thus increasing the pulse energy to approximately 0.3 mJ.

SHG experiments were performed with an unfocused laser beam, about 2 mm diameter, in transmission geometry. The beam was incident on the glass substrate of the film then passed through the film. The laser beam was *p*-polarized. A red cut-off filter was employed to eliminate spurious SHG signals generated by the optical setup before the sample. A sample film on an ITO-coated glass slide was mounted horizontally upon a temperature-controlled aluminium block equipped with a small hole. The fundamental laser beam was directed with a mirror through this hole to approach the film with the incidence angle of about 40 degrees. A wire spring attached to the metal block served as a ground electrode providing electrical connection and the grounding of the ITO layer.

The corona poling setup consisted of a stainless steel needle of the diameter about 0.45 mm with a sharp tip positioned about 2 cm above the film, directly over the laser beam spot. A negative DC voltage, 4–7 kV, was applied to the needle from a Hipotronix DC high voltage supply (Hubbel, model HD 100, series Hipot Tester). Alternately, a positive DC voltage was provided for a corona discharge from a Trimax Ionisation Tester (model G85A). The current level was about 1–4 μA during corona discharge. For most measurements the sample holder and the corona needle were kept in air, but occasionally the experiments were carried out in a box under nitrogen.

The intensity of the SHG signal, detected after filtering with the interference filter passing light of the 526.5 nm wavelength, was measured with a photomultiplier tube connected to one channel of a two-channel oscilloscope. The other channel was connected to a photodiode monitoring the intensity of the fundamental beam. The optical signals, and the film temperature measured by a thermocouple, were simultaneously monitored by a GPIB equipped computer with a data collection program. The data points were collected every 2 seconds. A 2-mm thick y-cut quartz crystal plate was used for callibrating of the SHG signals from the films.

RESULTS

Linear Optical Properties

The electronic absorption spectra of DR1-doped films of polycarbonate resin and of the titania/silica/hybrid polymer resin are shown in Figure 2. The wavelength of the absorption maximum of DR1, $\lambda_{\max}$ was at 490–492 nm in the PC host, 502–504 nm in the sol-gel hybrid organomineral host.

The spectra of the films were measured after corona poling followed by the chromophore orientation randomised on removal of the poling field (de-poling) at elevated temperatures. Absorption maximum of the processed films were shifted 2–4 nm to shorter wavelengths than in the fresh films. The decadic absorption coefficient, α_{10}, derived from the absorbance A, measured by the spectrophotometer, depended on the dye content in a film. $A = \log(I_o/I) = \alpha_{10}L$, where I_o denotes the intensity of light incident on the sample, I is the transmitted intensity, L is thickness of the film (μm). The absorption coefficient, ε_{10}, referring to the dye concentration c in the films ($\varepsilon_{10} = \alpha_{10}/c$) was about 0.1 μm^{-1} $wt\%^{-1}$ at $\lambda_{\max}$ for DR1 in the polycarbonate and the sol-gel films. The values of the absorption coefficients α, defined by $\ln(I_o/I) = \alpha L$ were used in evaluation of absorption corrections of second harmonic intensity and NLO parameters for the individual samples.

The linear optical properties of the films are listed in Table 1. The refractive indices of the unpoled films and the glass substrates at the fundamental wavelength (1053 nm) and the harmonic wavelength (526.5 nm) were derived from the experimental data, measured at several wavelengths (632.8 nm, 814 nm, 1064 nm), and extrapolated using a Sellmeier equation. These indices have been used in the calculations of the reflection and transmission coefficients (the Fresnel coefficients)

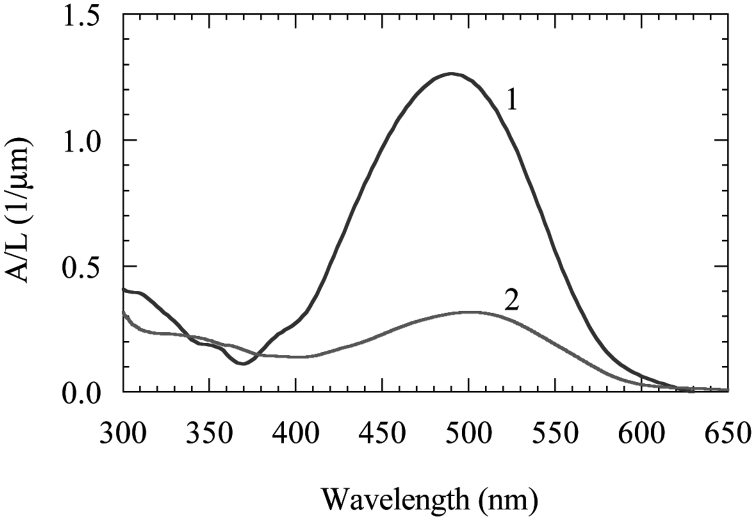

FIGURE 2 Absorption spectra (absorbance A divided by sample thickness L) of films of polycarbonate resin doped with 13 wt% of DR1 – curve 1, and of the titania/silica/hybrid polymer resin doped with 3 wt% of DR1 – curve 2.

required for the evaluation of the nonlinear coefficients d_{eff} and d_{ij} from the second harmonic power measured with the Maker fringes technique.

In Situ Second Harmonic Generation

The aim of this work was to align dipolar molecules of the nonlinear chromophore with a dc field in a non-centrosymmetric order in the polymer films, and to probe the orientation alignment with SHG. Our

TABLE 1 Absorption Coefficients α_{10}, α, and Refractive Index n in Films of Resins Doped with Disperse Red 1 (DR1) Dye

Host	DR1 conc. (wt%)	λ (nm)	α_{10} (μm^{-1})	α (μm^{-1})	n
Hybrid sol-gel	3	501 (max)	0.35	0.80	–
resin		526.5	0.31	0.70	1.6141
		1053	~0	~0	1.5885
Poly(bisphenol	13	490 (max)	1.26	2.91	–
A carbontate)		526.5	0.97	2.24	1.6658
resin		1053	~0	~0	1.6023

experimental optical setup allowed us to monitor the second harmonic intensity generated during corona poling of the films as a function of time, temperature and poling conditions. The polar ordering of dipoles was considered in terms of the rotation mobility of dipoles in amorphous polymers defined with the average rotation mobility parameter $\rho(T)$ [10] in Eq. (2). The parameter $\rho(T_1)$ can be estimated from the square root of the ratio of the intensity of second harmonic $I^{2\omega}(T_1)$, generated in the polymer at temperature T_1 to the intensity of second harmonic $I^{2\omega}(T_2)$ at high temperature T_2 [10]. At T_2, being higher than the glass transition temperature ($T_2 \gg T_g$), the dipoles are more free to rotate. Under the low field approximation Eq. (3) gives an experimental measure of the orientation ability of the dopant in films.

$$\rho(T_1) = \left(\frac{I_{33}^{2\omega}(T_1)}{I_{33}^{2\omega}(T_2 > T_g)}\right)^{0.5}\left(\frac{T_1}{T_2+\delta}\right) - \delta \tag{3}$$

where ${I_{33}}^{2\omega}$ is the second harmonic intensity polarized in the direction 3 generated by incident light I_3^{ω} polarized in the direction 3. The parameter $\delta = \gamma k T_1/\mu\beta$, where γ is the second hyperpolarizability, β is the first hyperpolarizability, μ is the dipole moment, k is the Boltzmann constant, is usually small and will be neglected in the analysis.

Figure 3 shows the temporal changes of the second harmonic signal, $P_{2\omega}$, normalised to the square of the power of the incident fundamental beam, P_{ω}^2, when the corona voltage was applied to the sol-gel film doped with 3 wt% of DR1.

In Figure 3 the poling experiment was performed on the film kept at room temperature (“cold poling”). We observed a fast increase of intensity of second harmonic due to the quick build-up of the nonlinear polarisation when the corona voltage was switched on followed by a plateau of the intensity level depending on the applied corona voltage. A fast decay of the intensity of second harmonic occurred when the corona was removed.

It is interesting to find out the parameters of the relaxation reorientation of the dye molecules in these two types of host polymers.

The second harmonic signals $(P_{2\omega},/P_{\omega,}^2)^{0.5}$ were normalised to the value of the second harmonic power taken at the last moment of poling, when the corona voltage was switched off. This power ratio is related to the ratio of the effective coefficients, d/d(0), where d(0) is taken as the d value at the end of the period of poling. Figure 4 shows the decay of the d coefficient observed in the 3 wt% DR1-doped sol-gel film after poling with the −7 kV corona voltage.

The decay in the curve was fitted with the relaxation parameters: the relaxation time constant τ of the decay of second-order nonlinear

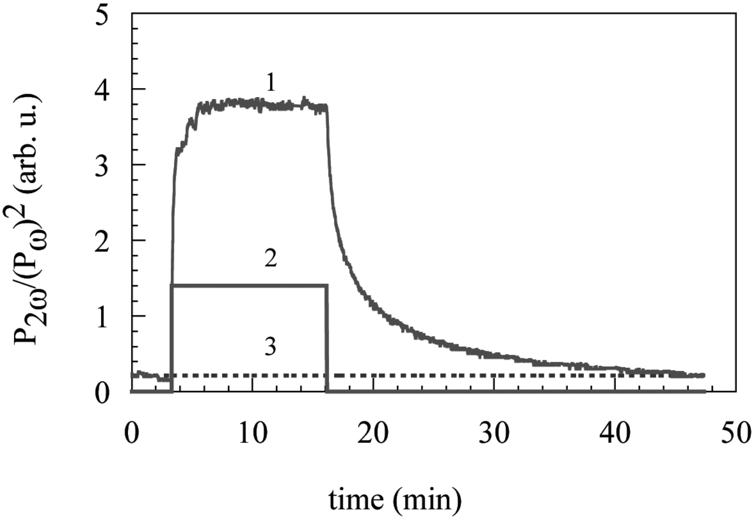

FIGURE 3 Monitoring of the second harmonic signal (curve 1), $P_{2\omega}$, normalized to the square of the power of the incident fundamental beam, P_{ω}^2, when the corona voltage (curve 2) – 7 kV was applied during poling (~13 min) at temperature 21°C (curve 3) to the sol-gel film, 1.9 μm thick, doped with 3 wt% of DR1. The decay time constant was found $\tau = 13$ min, b = 0.44.

optical susceptibility due to chromophore reorientation, and the distribution of the relaxation time constants given by b. We tried to evaluate them from fitting of the dependence of d/d(0) on time using a one-term stretch-exponential function [19,20] using Eq. (4a) transformed into a linear form in Eq. (4b):

$$\frac{d_{\text{eff}}(t)}{d_{\text{eff}}(0)} = \exp\left[-\left(\frac{t}{\tau}\right)^{b}\right] \tag{4a}$$

$$\log\left[-\ln\left(\frac{d_{\text{eff}}(t)}{d_{\text{eff}}(0)}\right)\right] = b\log\left(\frac{t}{\tau}\right) = b\log t - b\log\tau \tag{4b}$$

The linear dependence of log{–ln[d/d(0)]} on log(time), gives the b value from the slope, the τ value can be calculated from the intercept value. An instantaneous response and a longer time response have been observed. Figure 5 indicates that the decay of d/d(0) in the DR1-doped sol-gel film calculated in the coordinates of the Eq. (4b) can be approximated with a linear dependence only at a longer time scale.

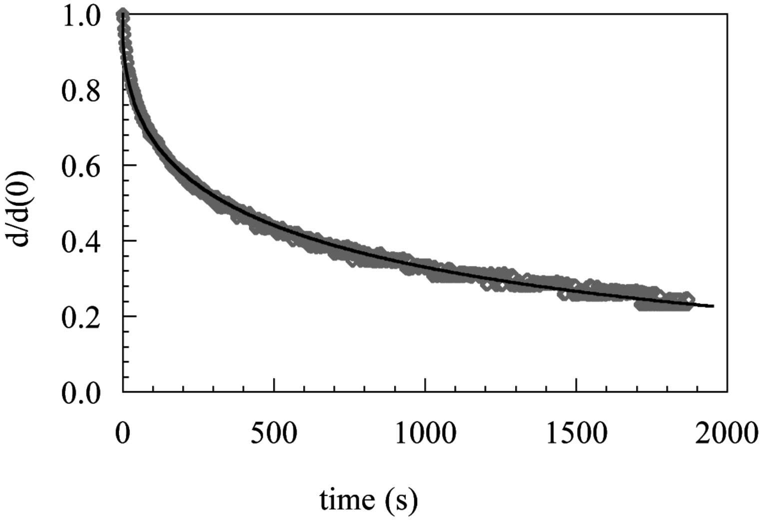

FIGURE 4 A decay of the normalized SHG d/d(0) coefficient after corona poling (−7 kV, 13 min, 21°C) of the sol-gel film doped with 3 wt% of DR1. The experimental data overlapped well with a stretch-exponential fitting curve having the parameters $\tau = 13$ min, b = 0.44.

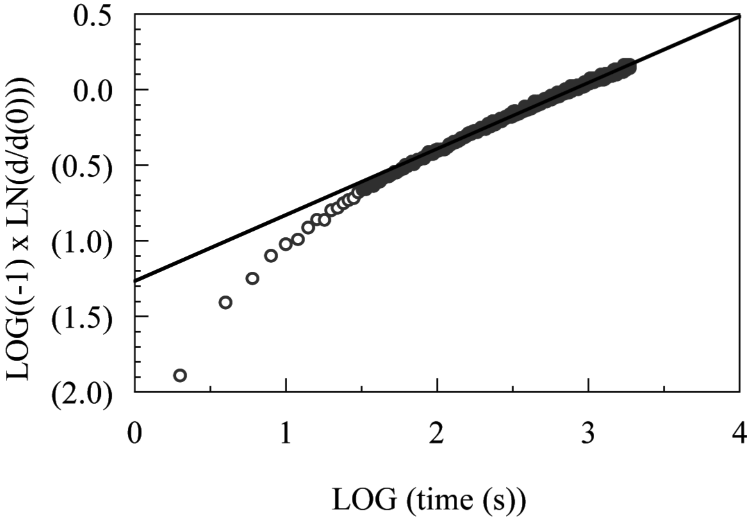

FIGURE 5 The long-time relaxation parameters ($\tau = 13$ min, b = 0.44) obtained in poling experiment at 21°C in a 3 wt% DR1-doped sol-gel film derived from the decay of normalized SHG coefficient d/d(0) fitted with a stretch-exponential function at the time scale bigger then 30–40 s.

The long-time relaxation process in the cold-poled DR1-doped sol-gel film was much faster (τ was found to be in the range of 5–12 minutes) than in the DR1-doped polycarbonate film, in which τ was in the range 50–150 minutes after cold poling.

Remarkable changes in the SHG process occurred in films poled at elevated temperatures. Figure 6 show the result of poling of the DR1-doped sol-gel resin when the film was heated up to 120°C then cooled down with the corona voltage kept on. A relatively fast decay of the d coefficient was still observed in the film at room temperature. The relaxation time τ was 195 min, when the corona voltage was removed at room temperature after hot poling.

The feature of the reduction of intensity of the second harmonic with increasing temperature of the film during poling was also observed in the DR1-doped polycarbonate resin, however the effect was much weaker. Figure 7 shows an example of this behaviour.

The high-temperature corona poling of the DR1-doped polycarbonate film, heated to about 120°C, produced a nonlinear polarization lasting much longer at room temperature. The estimated relaxation time τ at room temperature was of the order of years. The relaxation time became shorter when the sample was kept at higher temperatures: the τ value

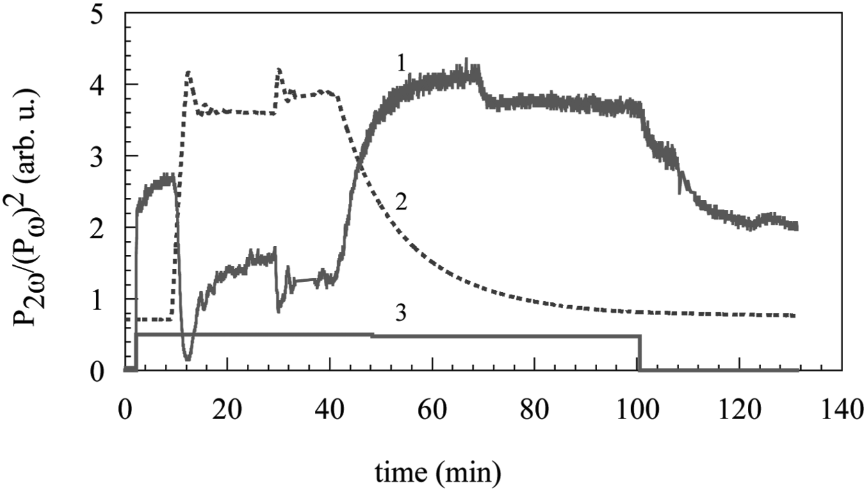

FIGURE 6 Variation of the second harmonic signal – curve 1, from a 3 wt% DR1-doped sol-gel film, 1.8 μm thick, during poling (–5 kV) at elevated temperature (115–120°C) and on cooling of the sample; curve 2 – temperature, curve 3 - corona voltage. The relaxation time τ was 195 min, b = 0.57 when the poling field was switched off at low temperature.

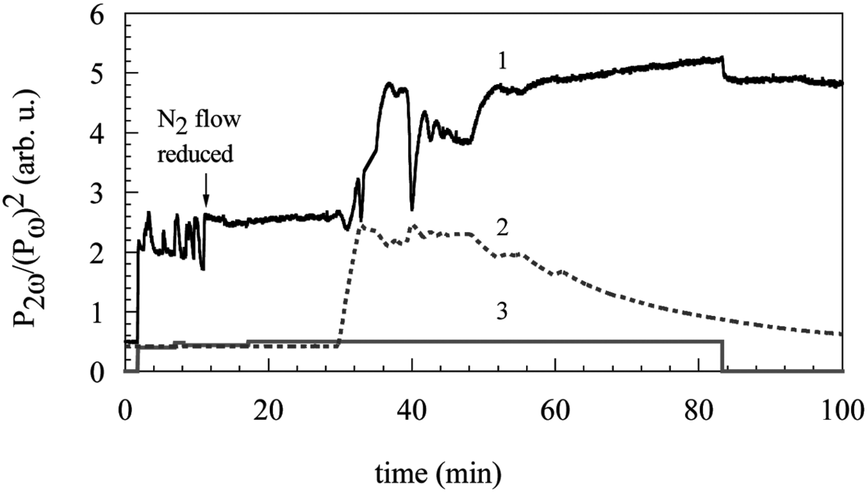

FIGURE 7 Variation of the second harmonic signal – curve 1, from a 13 wt% DR1-doped polycarbonate film, 0.8 μm thick, during corona poling (−5 kV) at room temperature, at high temperature (115–120°C), and on cooling of the sample; curve 2 – temperature, curve 3 – corona voltage.

was of the order of 2–4 days when the sample was kept without the field at 80°C, and about 30 min when the sample was kept at 95°C.

Second-Order NLO Coefficients

The second-order nonlinear optical coefficients d_{eff} and d_{ijk} were evaluated from the ratio of the second harmonic power measured in films to the signal obtained from a plane parallel slab of quartz crystal ($d_{11,9}$was taken as 0.5 pm/V) [1]. The d_{eff} for the films were calculated from Eq. (5) derived from theory of the Maker fringes technique [1].

$$(d_{\rm eff})^2 = \left(\frac{P_\omega^{\rm ref}/w_0^{\rm ref}}{P_\omega/w_0}\right)_{in}^2 \left(\frac{L_{\rm ref}}{L_f}\right)^2 \times \frac{T_\omega^{\rm ref}(0)T_{2\omega}^{\rm ref}(0)}{T_\omega^{(s,\phi,p)}(\theta^f)T_{2\omega}^{(s,p)}(\theta^f)} \frac{(P_{2\omega}^{(s,p)}(\theta^f))_{\rm out}}{(P_{2\omega}^{\rm ref}(0))_{\rm out}} \frac{(d_{\rm eff}^{\rm ref})^2}{F(L_f,\theta^f)} \tag{5}$$

The symbols used in Eq. (5) have the following meaning: ω is the light fundamental frequency, 2ω is the frequency of the second harmonic, the subscript f denotes a film quantity, ref – that of a reference sample, n is the refractive index of a medium, w_0 is the beam waist, s and p denote light beam polarizations. θ^f is the internal angle of refraction, which corresponds to the incidence angle θ of the fundamental beam on the sample through the nonlinear Snell's law [1]. We performed our calculations at the angle θ^{f} corresponding to the incident angle on the films, $\theta = 40^\circ$.

The coherence length $L_c^{\mathrm{ref}}(0)$ for the quartz reference at normal incidence was taken as the experimental value of 20.65 μm at the fundamental wavelength $\lambda_\omega = 1064\,\mathrm{nm}$ after Jerphagnon and Kurtz [14]. Other experimental data indicated 20.9 μm [21], 20.42 μm was calculated from refractive indices for quartz crystal, given in Ref. [21]. The coherence length of the materials at the wavelength of 1053 nm, derived from refractive indices of the films, was 4.2 μm in the PC film doped with 13 wt% DR1, and 10.3 μm the 3 wt% DR1-doped sol-gel film. The thicknesses of the films, L, were shorter than the coherence lengths, L_f was taken as equal to the optical path, $L_f = L/\cos\theta^{\mathrm{f}}$ at the incident angle.

The transmission coefficients t and the transmittance T of the interfaces were calculated from the Fresnel formulae [1] adapted for the geometry of the current experiment. $P_M^{(s,p)}(\theta')$ is the envelope of the second harmonic signal fitting the Maker fringes. It is related to the output second harmonic power $(P_{2\omega}^{(s,p)})_{\mathrm{out}}$ in Eq. (6) through the function $F(L_f,\theta)$, which accounts for the effect of absorption loss of the second harmonic power in light absorbing polymer films [1].

$$(P_{2\omega}^{(s,p)})_{\mathrm{out}} = P_M^{(s,p)} F(L_f, \theta) \tag{6}$$

The absorption correction factor F was calculated from relations given in Ref. [1]. The values of d_{eff} in the films were measured with the *p*-polarized fundamental and the *p*-polarized second harmonic (*p-p* polarization). The corona poled film with field applied normal to the plane of the film acquires symmetry axis in the film, and the point symmetry group is ∞mm ($C_{\infty v}$). Therefore, the poled polymer films, like 4mm and 6mm crystals, have nonzero tensor elements $d_{15} = d_{24}$, $d_{31} = d_{32}$, and d_{33}. The d_{eff} for a *p-p* polarization is related to the d_{ij} coefficients [1,11] through Eq. (7)

$$d_{\mathrm{eff}} = 2d_{15}\cos\theta_\omega \sin\theta_\omega \cos\theta_{2\omega} + (d_{31}\cos^2\theta_\omega + d_{33}\sin^2\theta_\omega)\sin\theta_{2\omega} \tag{7}$$

We assume the Kleinman symmetry, therefore $d_{15} = d_{31}$, and $d_{15}/d_{33} = 1/3$. The d_{33} coefficient was derived from the formula (8):

$$d_{33} = \frac{d_{\mathrm{eff}}}{\left[0.66\cos\theta_\omega \sin\theta_\omega \cos\theta_{2\omega} + (0.33\cos^2\theta_\omega + \sin^2\theta_\omega)\sin\theta_{2\omega}\right]} \tag{8}$$

TABLE 2 Second-Order NLO Coefficients, d, and the Average Rotational Mobility Parameter ρ(T) in Disperse Red 1-doped Films

Material	d_{eff} (pm/V)	d_{33} (pm/V)	ρ(294 K)
3 wt% DR1 in sol-gel resin	8.7 (7.7 in cold poling)	22 (19 in cold poling)	–
13 wt% DR1 in polycarbonate resin	26 (20 in cold poling)	63 (50 in cold poling)	0.8

The θ angles are the internal refraction angles in a film. The values of d_{eff} and d_{33} coefficients obtained during poling of the films are listed in Table 2.

DISCUSSION

The *in situ* dc electric field induced second harmonic generation provides valuable insight into the build-up of polar orientation and stability of alignment of NLO chromophores. The SHG technique is useful for screening the NLO polymers with short and long orientation relaxation time.

The polar alignment of the chromophores must be preserved at operating temperatures in order to retain the macroscopic nonlinearity of the system and show NLO effects. Generally, polymers with covalently attached NLO chromophores in a side-chain are regarded as more stable (less susceptible to thermal relaxation) after poling than dye-doped guest-host NLO materials. However, we found the stability of second-order NLO properties of PMMA bearing a relatively long side-chain chromophore to be quite low [22]. Our studies aim at an efficient and stable NLO system, which has a high glass transition temperature, and low ability for chromophore reorientation after poling. The polymers studied here formed different host environments for the relatively large DR1 molecule. We observed a high value of second harmonic intensity induced by poling at room temperature of the DR1-doped sol-gel film. The signal decayed quickly on removing of the poling field. This indicates a highly polar ordering, and a high mobility of the dopant, which may be related to a large excess free volume for rotation [10] in this matrix. The sol-gel resin was only slightly thermally cross-linked before the corona poling experiment. A more stable performance of this material is expected when poling is followed by efficient thermal or photo-crosslinking. However, the fast relaxation behaviour may be interesting for application in photorefraction phenomena.

Interesting features have been observed in the temporal evolution of the second harmonic intensity during corona poling of the films at room temperature and during a simultaneous poling and heating of these two materials to a higher temperature, about 120°C. The SHG data obtained on two types of our host polymers indicate that the process of orientation of the DR1-dopant molecules depends in a complicated way on temperature and the poling electric field. The maximum of the second harmonic intensity in the DR1-doped sol-gel resin matrix could not be achieved at higher temperatures, rather opposite, the second harmonic signal and the NLO coefficients decayed in the film when it was kept under poling field at elevated temperatures. The T_g of the sol-gel resin (undoped) was found to be near 60°C. It means that a large number of dye molecules should be oriented with the applied external field at elevated temperatures. The reduction of SHG with increasing temperature can be related to an increase of the material conductivity, which facilitates current flow through the film, and a reduction in the voltage drop across the film. Thus, the corona discharge becomes less effective for the orientation of molecules in the sol-gel film at high temperatures.

An important attractive feature of the polycarbonate host was its high value of the glass transition temperature ($T_g = 150°C$) in neat polymer. The non-centrosymmetric alignment of chromophores can last longer in a PC polymer than e.g. in PMMA. However pre-glass transition phenomena, which are known to occur in polycarbonate may also affect the dye orientation order in this host. The orientation mobility of DR1 in PC was deduced from the average rotational mobility parameter $\rho(T)$ measured with the $\chi^{(2)}$ at 294 K relative to $\chi^{(2)}$ at temperatures above T_g. The ρ parameter equal to 0.8, found in our polycarbonate resin film (weight average molecular weight MW 64,000) doped with 13 wt% DR1, is different from the value of about 0.06 found in a film of polycarbonate (MW = 38100, $T_g = 65°C$) doped with 5 wt% DR1 in Ref. [10]. This difference, being attributed to higher mobility of the dye, may indicate the presence of larger voids enabling rotation of the dye molecules in our material and allowing for faster orientation relaxation.

CONCLUSIONS

The *in situ* dc electric field induced SHG technique is very useful for screening the NLO polymers with short and long orientation relaxation times. The relaxation parameters were derived here from a simple one-term stretch-exponential function; however, a more complex function is required to fit the decay of $\chi^{(2)}$ in poled films. A short relaxation time $\tau \sim 5$–12 min of decay of SHG was found in films of newly synthesised sol-gel hybrid polymer doped with DR1, corona-poled at room temperature, $\sim$200 min after high-temperature poling. A longer relaxation time $\tau \sim 50$–150 min was found in the DR1-doped polycarbonate films poled at room temperature, the τ value was of the order of years after high-temperature poling.

Large values of the (resonantly enhanced) second-order NLO coefficients d_{eff}, and d_{33} were found in the DR1-doped materials. A high value of the rotation mobility parameter ρ was found in DR1/PC film. The ρ parameter could not be derived for the sol-gel resin due to a spurious effect of a strong reduction of the second harmonic intensity, which occurred during corona poling of the material at elevated temperatures.

REFERENCES

[1] Sutherland, R. L., McLean, D. G., & Sean, K. (2003). *Handbook of Nonlinear Optics. Second Edition, Revised and Expanded*, Marcel Dekker: New York.

[2] Samoc, A., Samoc, M., Prasad, P. N., & Krajewska-Cizio, A. (1992). *J. Opt. Soc. Am. B*, *9*, 1819.

[3] Samoc, A., Samoc, M., Kohler, D., Stahelin, M., Funfschilling, J., & Zschokke-Granacher, I. (1992). *Mol. Cryst. Liq. Cryst. S&T, Section B: Nonl. Opt.*, *2*, 13.

[4] Kelly, J. F., Krausz, E. R., Samoc, A., Samoc, M., & Willis, A. C. (2002). *Aust. J. Chem.*, *55*, 709.

[5] Samoc, A., Samoc, M., Luther-Davies, B., Kelly, J., Krausz, E., & Willis, A. (2004). *Mol. Cryst. Liq. Cryst.*, *415*, 179.

[6] Eich, M., Sen, A., Looser, H., Bjorklund, G. C., Swalen, J. D., Twieg, R., & Yoon, D. Y. (1989). *J. Appl. Phys.*, *66*, 2559.

[7] Mortazawi, M. A., Knoesen, A., Kowel, S. T., Higgins, B. G., & Dienes, A. (1989). *J. Opt. Soc. Am. B*, *6*, 733.

[8] Williams, D. (1987). In: *Nonlinear Optical Properties of Organic Molecules and Crystals*, Chemla, D. S. & Zyss, J. (Eds.), Academic Press: Orlando, Fla., Vol. 1, 405.

[9] Singer, K. D., Kuzyk, M. G., & Sohn, J. E. (1987). *J. Opt. Soc. Am. B*, *4*, 968.

[10] Boyd, G. T., Francis, C. V., Trend, J. E., & Ender, D. A. (1991). *J. Opt. Soc. Am. B*, *8*, 887.

[11] Hayden, L. M., Sauter, G. F., Ore, F. R., & Pasillas, P. L. (1990). *J. Appl. Phys.*, *68*, 456.

[12] Dureiko, R. D., Schuele, D. E., & Singer, K. D. (1998). *J. Opt. Soc. Am. B*, *15*, 338.

[13] Page, R. H., Jurich, M. C., Reck, B., Sen, A., Twieg, R. J., Swalen, J. D., Bjorklund, G. C., & Willson, C. G. (1990). *J. Opt. Soc. Am. B*, *7*, 1239.

[14] Jerphagnon, J. & Kurtz, S. K. (1970). *J. Appl. Phys.*, *41*, 1667.

[15] Herman, W. N. & Hayden, L. M. (1995). *J. Opt. Soc. Am. B*, *12*, 416.

[16] Luo, X., Zha, C., & Luther-Davies, B. (2005). *J. Non-Cryst. Solids*, *351*, 29.

[17] Kolev, V. Z., Lederer, M., Luther-Davies, B., Tan, H., & Jagadish, C. (3–6 Dec. 2001). In: *Australasian Conference on Optics, Lasers and Spectroscopy*, MacGillivary, W., Rubinsztein-Dunlop, H., Harvey, M., & Gagen, M. J. (Eds.), University of Queensland: Brisbane, Australia, 137.

[18] Lederer, M. J., Kolev, V., Luther-Davies, B., Tan, H. H., & Jagadish, C. (2001). *J. Phys D: Appl. Phys.*, *34*, 2455.

[19] Hooker, J. C. & Torkelson, J. M. (1995). *Macromol.*, *28*, 7683.

[20] Strutz, S. J., Brower, S. C., & Hayden, L. M. (1998). *J. Polym. Sci.: Part B: Polym. Phys.*, *36*, 901.

[21] Bosshard, C., Knoepfle, G., & Guenter, P. (1992). *J. Appl. Phys.*, *71*, 1594.

[22] Samoc, A., Luther-Davies, B., Samoc, M., Wong, M. S., Krolikowska, R. M., Martin, T. M., MacLeod, C. J., Freydank, A. C., Peng, G.-D., & Whitbread, T. (2002). *Proc. SPIE*, *4798*, 87.